RSC Advances

ROYAL SOCIETY OF CHEMISTRY

www.rsc.org/advances

Journal Name

Dynamic Article Links ►

Cite this: DOI: 10.1039/c0xx00000x

www.rsc.org/xxxxxx

ARTICLE TYPE

Improvement of Dye-Sensitized Solar Cells' Performance through Introducing Different Heterocyclic Groups to Triarylamine Dyes

Ze-Min Ju,[a] Hai-Lang Jia,[a] Xue-Hai, Ju,[b] Xing-Fu Zhou[c], Zhi-Qiang Shi,[a] He-Gen Zheng*[a] and Ming-Dao Zhang*[a,d]

Received (in XXX, XXX) Xth XXXXXXXXX 201X, Accepted Xth XXXXXXXXX 201X

DOI: 10.1039/b000000x

This paper focuses on the structure modification of triphenylamine dyes for efficient dye-sensitized solar cells (DSSCs). Three D-D-π-A dyes (TTR1-3), with triphenylamine moiety and its derivatives as electron donor, thiophene ring as π-bridge, and 2-(1,1-dicyanomethylene)rhodanine (DCRD) as electron acceptor, were synthesized and fully characterized. Nanocrystalline TiO_2-based DSSCs were fabricated using these dyes to investigate the effect of different donor groups introduced into triphenylamine on their photovoltaic performances. The overall power conversion efficiency (PCE) of DSSCs based on TTR1-3 with chenodeoxycholic acid (CDCA) coadsorbant are 5.20%, 5.71% and 6.30%, respectively, compared to 6.62% achieved with N719. Introduced heterocyclic group with alkyl lain into triphenylamine decreased dye absorbed amount but significantly improved the value of the open circuit voltage (V_{oc}) and the short-circuit photocurrent (J_{sc}), which result from the fact that they can effectively suppress the charge recombination and prevent aggregation between adjacent molecules on TiO_2. We also researched the effect of sensitization way for single dye on their photovoltaic performances. The PCEs of DSSCs soaked for 32 h increase slightly than those of DSSCs soaked for 16h, which result from the adsorption quantity on TiO_2 surface. We found that, with soaking twice in 32 h, the J_{sc} and V_{oc} were both obviously improved compared with soaking once in 32 h. These results provide a new approach for enhancing the photovoltaic performances of DSSCs based on single dye.

1.Introduction

Dye-sensitized solar cells (DSSCs), firstly developed by Grätzel in 1991,[1] have attracted tremendous interest during the past two decades as one of the promising candidates for low-cost and clean solar energy conversion devices. In particular, their good performances under low light intensity, and the ability to fabricate device with various colors, support their application as portable energy devices. A typical DSSC consists of three components: a dye-sensitized nanocrystalline TiO_2 photoanode, redox electrolyte such as an iodide/triiodide, and a counter electrode (CE).The complete basic working principles of a DSSC can be found everywhere.[2]

Optimization of DSSCs efficiency can be addressed in a variety of ways, such as designing different sensitizers with different chemical structures[3,4], and exploiting different electrolytes including ionic liquids and solid state hole conducting materials[5,6]. For many years, ruthenium based complexes were the "champion" dyes of DSSCs and some of them were distinguished by achieving more than 11% efficiency[7]. However, ruthenium cannot be considered "earth abundant materials" and, thus, it is desirable to look for alternative dyes. In order to get high conversion efficiency and low cost DSSCs, much effort has been dedicated to designing and synthesizing dyes such as zine porphyrin. After appropriate tailoring of the chemical structure and employment of a cobalt electrolyte, the porphyrin dye YD2-o-C8 with Y123 coadsorbant showed PCE of up to 12.3% under standard conditions (AM 1.5 G, 100 $mWcm^{-2}$ intensity)[8] which was further improved to 13% utilizing SM315[9]. However, porphyrins usually require complicated synthetic strategies with relatively low yields, especially when an anchoring function and a redox group have to be introduced at specific positions. Metal-free organic dyes as sensitizers in DSSCs have drawn widespread academic and commercial attention because of their high molar extinction coefficient and easily adjustable spectral response. Recently, a number of novel metal-free organic sensitizers, such as triphenylamine[10], indoline[11], perylene[12], carbazole[13], tetrahydroquinoline[14], phenothiazine[15] and fluorene dyes[16], have been investigated and applied in DSSCs successfully.

In this paper, three novel triphenylamine sensitizers TTR1-3 have been designed and synthesized. As donors, triphenylamine and its derivatives[10,17-21] have shown promise in the development of DSSCs, owing to: 1) three benzene rings of triphenylamine have high activity, so the different functional groups are easy to be introduced. 2) three non-coplanar phenyl having propeller structure which results in large steric hindrance can effectively prevent aggregation between adjacent molecules on TiO_2 surface. 3) triphenylamine which possess high molar extinction coefficient and strong electron donating ability is prone to electron delocalization. Compared with alkyloxy chain, heterocyclic group, such as thienyl, 3,6-di-tert-butyl-9H-

carbazolyl and 5-hexylthiophen-2-yl which are introduced into triphenylamine in this paper can bring wide absorption spectra and prevent the dye aggregation on TiO_2 surface. 2-(1,1-dicyanomethylene)rhodanine (DCRD) is chosen as electron acceptor, which can not only bring wide absorption spectra, but also maintain excellent electron injection efficiency owing to its special characteristics. What's more, the O and N on the rhodanine unit can both form strong chelating bonds with Ti cations, furnishing enhanced stability of the dyes in comparison with COOH anchor.[22-24] To our knowledge, this is one of few reports of dyes with DCRD as electron acceptor showing higher efficiency. The molecular structures of TTR1-3 which possess the structure of donor-donor-π-bridge-accepter (D-D-π-A) are shown in Scheme 1, where the π-bridge is the thiophene.

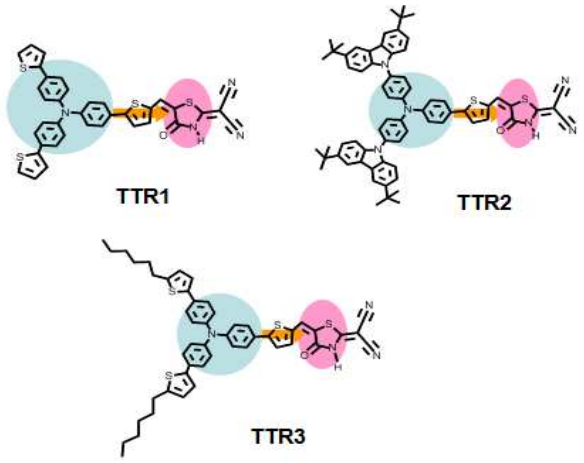

Scheme 1 Molecular structures of TTR1-3.

These three dyes were used to manufacture dye-sensitized solar cells with chenodeoxycholic acid (CDCA) coadsorbant. The differences of the photovoltaic performances based on these dyes have been analyzed by UV-vis absorption, cyclic voltammogram, and electrochemical impedance spectroscopy (EIS). We showed that by incorporating two heterocyclic groups with large steric hindrance into the triphenylamine-based dyes, the efficiency can be improved obviously. Compared to 6.62% achieved with N719, the overall PCE of the DSSCs based on TTR1-3 dyes are 5.20%, 5.71% and 6.30%, respectively. We also studied the effect of sensitization way on the performance of DSSCs. The improvement of PCE is realized through re-sensitization, which provides a new method to improve the PCE for single dye.

2. Experimental

2.1 Synthesis of dyes

In the previous studies of sensitizers, the tuning of donor and acceptor units has been well demonstrated to extend the absorption spectrum, adjust the HOMO and LUMO levels, and realize the intramolecular charge separation. Synthetic routes of the fragment are described in Scheme S1, which are according to the methods reported[25-27], respectively. As depicted in Scheme S2, the synthesis of TTR1, TTR2, and TTR3 were started from tris(4-bromophenyl)amine, which was converted into corresponding intermediates **7**, **9**, and **12** by Suzuki coupling reaction with 2-thiopheneboronic acid and 5-formyl-2-thiopheneboronic acid, respectively. Intermediate 5-(4-(bis(4-(3,6-di-tert-butyl-9H-carbazolyl)phenyl)amino)phenyl)thiophene, **10**, was achieved from **9** and **1** by Suzuki cross coupling reaction, and then, formylated to give the corresponding aldehyde (**11**). Aldehyde **8** and **13** were obtained by corresponding Suzuki cross coupling. Finally, the Knoevenagel reaction was carried out with 2-(1,1-dicyanomethylene)rhodanine under refluxed condition to directly produce the target dye (TTR1-3). The preparation details of TTR1-3 are presented in the ESI.

2.2 Optical spectroscopy

UV-vis absorption spectroscopy of dyes was investigated with a Shimadzu UV-3600 spectrometer in the liquid phase. To obtain the absorption spectra of the dyes on TiO_2, transparent 13 μm-thick TiO_2 films were prepared as is described in device fabrication in the ESI. The UV-vis absorption spectra of dyes sensitized on TiO_2 were recorded with a Shimadzu MPC-3100 spectrometer for the solid phase at room temperature.

2.3 Electrochemistry and measurement of dye adsorbed amounts

A xenon light source (Oriel) was used to give an irradiance of 100 mW cm^{-2} at the surface of a testing cell using a keithley 2400 source meter. The measurement delay time was fixed to 40 ms with 100 measurement points scanning from V_{oc} to J_{sc}.[28] For the setup used in our measurements, there was no hysteresis in the *J-V* curves when reversing the scan direction.

The incident photon-to-current conversion efficiency (IPCE) of the DSSCs was measured by a DC method. The light source was a 300 W xenon lamp (Oriel 6258) coupled with a flux controller to improve the stability of the irradiance. The light passed through a monochromator (Cornerstone 260 Oriel 74125) to select a single wavelength with a resolution of 10 nm. The monochromatic light beam was then focused on the active region of the device. Light intensity was measured by a NREL traceable Si detector (Oriel 71030NS) and the short circuit currents of the DSSCs were measured by an optical power meter (Oriel 70310).

Quasi-reversible oxidation and reduction waves were recorded using a Chenhua CHI660D model Electrochemical Workstation (Shanghai), while Electrochemical Impedance Spectroscopy was carried out using a Chenhua CHI660I model Electrochemical Workstation (Shanghai).

To estimate the adsorbed amounts of dye on the TiO_2 film, the sensitized 6×6 mm electrodes were separately immersed into a 0.1 M NaOH solution in a mixed solvent (water : N,N-dimethylformamide = 1 : 1), which resulted in the desorption of each dye. The absorbance of the resulting solution was measured with a Shimadzu UV-3600 spectrometer.

2.4 Theoretical calculations

All calculations were performed in the Gaussian 09 program package.[29] Without any symmetrical constraints, the geometrical structures of TTR1, TTR2 and TTR3 were optimized by the DFT-B3LYP/LanL2MB level (a semiempirical method).[30] Incorporating the optimized model in the ZINDO method,[31] we

calculated excitation energies and oscillator strengths of TTR1, TTR2 and TTR3.

3. Results and discussion

3.1 Absorption Spectra

The UV-visible absorption spectra of TTR1-3 in the dichloromethane solution are displayed in Fig. 1a, and the corresponding data are summarized in Table 1. Owing to their similar structures, all the triphenylamine dyes exhibit strong absorption peaks located in the ranges of 300-400 nm and 450-560 nm, which are attributed to π-π* electron transition and intramolecular charge transfer (ICT) transition from the triphenylamine moiety (donor) to DCRD (acceptor), respectively. The values of the molar extinction coefficient at the maximum absorption wavelength (λ_{max}) for the those dyes are in the range of 2.7-3.1 × 10^4 M^{-1} cm^{-1}, of which the value of TTR2 is larger than those of the other two dyes in the range 450-560 nm. As expected, the UV-visible absorption bands of the three dyes are sensitive to substituents on the periphery of the triphenylamine.

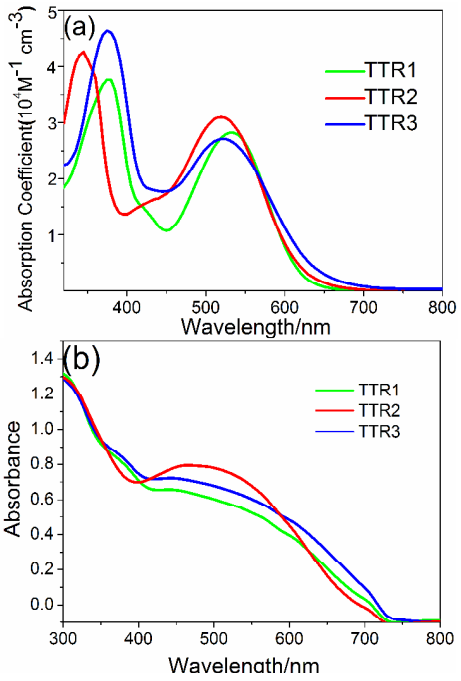

Fig. 1 (a) Electronic absorption of TTR1, TTR2, and TTR3 dissolved in dichloromethane. (b) Electronic absorption of TTR1, TTR2, and TTR3 absorbed on TiO_2 thin film.

All of the bands of TTR1-3 are broadened significantly in comparison with the reference triphenylamine dye RD-II[24], the absorption spectra of TTR3 extends to 730 nm. The maximum absorption wavelength (λ_{max}) for TTR1-3 are 535, 521 and 526 nm in the range 450-560 nm, respectively, which are about 10 nm red-shifted than that of the RD-II which contains octyloxy units on the periphery of the triphenylamine. The increase in red-shift of the absorption band is possibly due to the electronic effect of the heterocyclic groups which can prolong the π-conjugation's length and amount of dyes molecules. This result confirms that the heterocyclic groups appended on triphenylamine have positive effect on improving the UV-vis absorption of the triphenylamine dyes.

Fig.1b shows the absorption spectra of the three dyes adsorbed on a transparent TiO_2 film. Compared with the spectra in dichloromethane solution, a blue-shift and broadening of the absorption peak was observed in all the dyes on TiO_2 surface, which can be attributed to the formation of deprotonation and H-aggregate.[32] Such spectral broadening allows the dye molecules to harvest visible light more efficiently. As shown in Fig. 1b, when the dyes were adsorbed on TiO_2 surface, TTR2 has a larger absorbance value than TTR1 and TTR3 in the range 430-570 nm, which is similar to the spectra in dichloromethane solution.

3.2 Theoretical Approach

To gain insight into the geometrical and electronic properties of the three sensitizers, density functional calculations were conducted using the Gaussian 09 program package at the B3LYP/LanL2MB level. It can be clearly found that, the HOMO of these compounds is populated over the substituted triarylamine moieties and the linked heterocyclic groups and the LUMO is delocalized over the DCRD group (electron acceptor), facilitating electron transfer from the excited state to the conduction band of TiO_2. Furthermore, the presence of strong electron density relocation between HOMO and LUMO supports the occurrence of an ICT transition in the UV−vis spectra.[33]

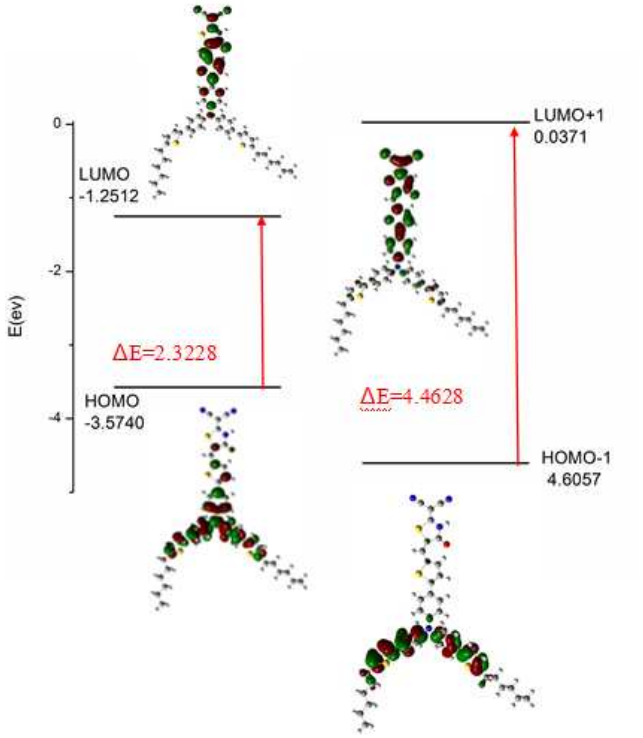

Fig. 2 Calculated HOMO, HOMO-1, LUMO and LUMO+1 levels for TTR3.

Time-dependent density functional theory (TDDFT) is used to analyze the excitation pathways and understand the injection process under different portions of sunlight irradiation.[34] Taking TTR3 for example, the observed two bands in absorption spectra are caused by several kinds of electron excitation. The low-energy band located at 526 nm is ascribed to HOMO→LUMO transition and the UV band around 375 is composed of HOMO→LUMO+1 and HOMO−1 →LUMO. Obviously, most transitions move excited electrons to LUMO and LUMO+1orbitals; hence, checking the electron distribution of these orbits is pivotal for evaluating electron injection in view of orbital overlap between sensitizer and TiO_2. Density functional theory (DFT) calculation on TTR3 indicates that the electrons of both LUMO and LUMO+1 are delocalized over the π-A moiety with a large composition on the anchoring group (Fig. 2), where the electron is close to the TiO_2 surface and can be smoothly injected into the CB of the TiO_2 semiconductor. The phenomenon of TTR3 is similar to those of TTR1 and TTR2 (Fig. S1-S2). Therefore, photons from each of the two absorption bands are useful for electron injection and photovoltaic conversion.

3.3 Infrared spectroscopy

We set out to confirm the nature of the surface attachment of the dyes by interrogating the binding modes through diffuse reflectance IR Fourier transform spectroscopy (DRIFTS) experiments. The spectra for the dyes attached (TTR + TiO_2) and unattached (TTR) to TiO_2 are presented in Fig. S3-S5. The spectra of TTR + TiO_2 clearly indicate the absence of the N-H stretching modes (ν_{N-H}) at 3200 cm^{-1} that are present for TTR, as the amide group can bond to form dimers by intermolecular hydrogen bonding. At the same time, the characteristic bands for the cyano group (C≡N) were clearly observed at 2205 cm^{-1}. For the dye powder, the frequency of carbonyl (C=O) stretching vibration and N-H bending vibration (δ_{N-H}) of the rhodanine were also raised to 1710 and 1646 cm^{-1} owing to the strong electron-withdrawing property of dicyanomethylene group, though the C=O and N-H absorption of amides usually occur at 1650 and 1570 cm^{-1}, respectively.[20] When the dyes were adsorbed on TiO_2 surface, the peak for cyano group remained detected at the same frequencies, while the absorption for ν_{N-H}, δ_{N-H}, and the C=O stretching bands disappeared. At the same time, two new bands emerged at around 3305 and 1636 cm^{-1}, which can be attributed to the characteristic absorption of hydroxy groups. The presence of O-H vibration may be due to the residual $Ti(OH)_2$ present in the powder. Based on the DRIFTS, it is considered that the DCRD moiety can chelate to TiO_2 like Fig.7b.

3.4 Electrochemical Properties

To determine the oxidation potential of the organic dyes and thermodynamically evaluate the possibility of sensitizer regeneration, cyclic voltammogram (CV) was carried out in a typical three-electrode electrochemical cell with TiO_2 films stained with sensitizer as the working electrode, Pt wire as the counter electrode, and Ag/Ag^+ as the reference electrode dipped in a solution of tetrabutylammonium hexafluorophosphate (0.1 M) in water-free dichloromethane at a scan rate of 50 mV s^{-1} at room temperature, and the corresponding data are summarized in Table 1.

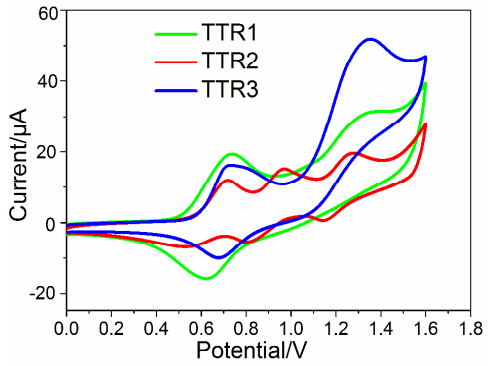

Fig. 3 Cyclic voltammogram of the oxidation behavior of the dyes.

Table 1 Optical and electrochemical properties data of TTR1, TTR2 and TTR3.

Dye	λ_{max} [nm] [a] (ε,10^4Lmol^{-1}cm^{-1})	λ_{max} [b] [nm]	E_{ox} [V] [c] (vs.NH)	E_{0-0} [d] [eV]	E^*_{ox} [V] [e] (vs.NH)
TTR1	535(2.82)	475	0.75	1.85	-1.10
TTR2	521(3.09)	492	0.72	1.80	-1.08
TTR3	526(2.71)	460	0.73	1.72	-0.99

[a] Absorption maximum in dichloromethane solution (3×10^{-5} M).

[b] Absorption maximum on 8 μm TiO_2 transparent films.

[c] The ground-state oxidation potentials of dyes were measured in a dichloromethane with 0.1 M tetra-n-butylammonium hexafluorophosphate ($TBAPF_6$) as electrolyte (Pt working electrode, SCE reference electrode calibrated with Ag/Ag^+ as an external reference, Pt counter-electrode).

[d] $E_{0-0}$was estimated from the absorption thresholds from UV-Vis absorption spectra of the dyes.

[e] E_{ox}^* was calculated as E_{ox} - E_{0-0}.

As shown in Fig.3, the TTR1 and TTR3 exhibit similar profile because of their similar structures, while there is a new oxidation peak for TTR2, which may results from the oxidation of carbazole fragment. Zero-zero excitation energy (E_{0-0}) estimated from the absorption onset[35] and the ground-state oxidation potential (E_{ox}) were used to calculate the excited-state oxidation potential (E_{ox}^*= E_{ox} - E_{0-0}). On the one hand, the deduced E_{ox}^* values of TTR1-3 which are similar to the experimental data (Fig.S6) are more negative than the conduction band edge of the TiO_2 (-0.5 V vs NHE),[35] indicating that the electron injection process should be energetically favorable. On the other hand, the E_{ox} (Table 1) of these three dyes are more positive than the redox potential of the I^-/I_3^- couple (0.4 V *vs* NHE)[32] suggesting that the oxidized dyes should be able to accept electrons from I^- thermodynamically for effective dye regeneration. Consequently, all dyes have enough thermodynamic driving forces for efficient DSSCs using nanocrystalline TiO_2 photoanode and I^-/I_3^- electrolyte.

3.5 Photovoltaic performance of DSSCs.

These three dyes were used to manufacture dye-sensitized solar cells in the presence of chenodeoxychlic acid (CDCA). The devices employed FTO glass anchored dye-loaded TiO_2 nanoparticles film as positive electrode, platinum-coated glass as counter electrode, and a solution of 0.6 M DMII, 50 mM LiI, 30 mM I_2, 0.5 M tert-butylpyridine and 0.1 M GuNCS in acetonitrile and valeronitrile (85 : 15) as the electrolyte. Photocurrent-voltage (*J-V*) curves for the DSSCs were recorded under irradiation of AM 1.5G full sunlight (100 mW/cm^2) and presented in Fig.4a. The exact results are summarized in Table 2.

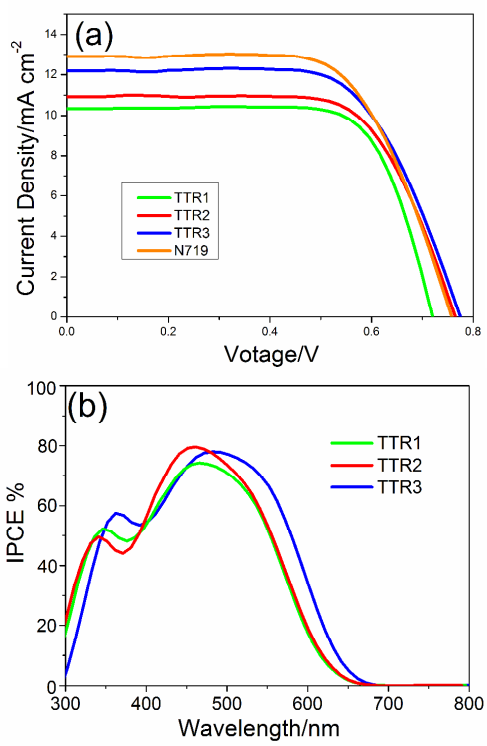

Fig. 4 (a) Photocurrent density-voltage curves for the DSSCs based on TTR 1-3 under irradiation of AM 1.5G full sunlight. (b) IPCE of DSSCs based on TTR1-3.

Table 2 DSSC performance parameters of TTR1, TTR2 and TTR3.[a]

Dye	V_{oc}(V)	J_{sc}(mA cm^{-2})	*F.F.%*	η%
TTR1	0.717	10.352	70	5.196
TTR2	0.762	10.978	68	5.714
TTR3	0.771	12.204	67	6.304
N719	0.754	12.909	68	6.619

[a]The photocurrent–voltage characteristics were measured with coadsorbent (10 M CDCA) for 13 μm thick TiO_2 film with liquid electrolyte (0.05 M I_2, 0.1 M LiI, 0.1 M DMPII, and 0.5 M TBP) at full sunlight (AM1.5G, 100 MWcm^{-2}).

As depicted in Fig. 4a, the values of the open-circuit voltage (V_{oc}) of TTR2 and TTR3 are superior to TTR1, which may be attributed to reduced charge recombination between injected electrons and electron acceptors (I_3^-) in the electrolytes. Introduced large functional groups into triphenylamine can effectively prevented I_3^- from approaching the TiO_2 surface. The values of short-circuit current (J_{sc}) for the three dyes are in the order of TTR1 < TTR2 < TTR3 and, specifically, the corresponding PCE (η) values are 5.20%, 5.71%, and 6.30%, respectively, and the value of TTR3 is closed to that of N719. The improvement of PCE from TTR1 to TTR3 is mainly assigned to the increase in the J_{sc}, which is partly due to different steric hindrance for three dyes. Compared with TTR1, TTR2 and TTR3 are provided with large steric hindrance, thus, they can effectively prevent aggregation between adjacent molecules on TiO_2 and suppress the charge recombination between the dye cation and the semiconducting oxide electrode. The absorption spectrum can also explain why the values of J_{sc} are different. As shown Fig.1a, compared with TTR2, TTR3 possesses a broader absorption band which indicates the superior ability of light harvesting at longer wavelength regions, so the J_{sc} value of TTR3 is larger than that of TTR2. The smallest J_{sc} value of TTR1 is mainly because of its weaker and narrower UV-vis absorption. So, the above results directly demonstrate that the photovoltaic performances of triphenylamine dye can be improved after introducing heterocycle moiety which leads the π-conjugation's length and amount to enlarge.

The IPCE spectra of the DSSCs employing TTR1, TTR2 and TTR3 are shown in Fig. 4b. IPCE curves of three triphenylamine dyes have similar profiles. IPCE values of TTR3 exceed 60% from 420 to 560 nm, with a maximum value (79.0%) at 480 nm leading to the highest J_{sc}. The higher IPCE value of the DSSC based on TTR2 in the range of 420-475 nm is probably due to a lower energy gap between the LUMO (Fig. S2 in the ESI) level of TTR2 and the conduction band edge of TiO_2, which leads to an increased electron injection efficiency compared with TTR1 and TTR3. This also may due to the existence of carbazole donor group, while TTR1 and TTR3 possess the thiophene donor group. Among all the dyes, IPCE value of TTR1 is lower than those of TTR2 and TTR3, and spectral response of TTR1 is also inferior to other dyes. Thus, TTR1 gives rise to a lower light harvesting efficiency, resulting in the smallest J_{sc}.

3.6 Electrochemical impedance spectroscopy

The high photocurrent of DSSCs based on TTR2 and TTR3 is not difficult to understand from their broad and high IPCE response. In contrast, the insight into their high V_{oc} (about 50 mV higher than the TTR1) is very worthy of investigation. For well-operational DSSCs, the V_{oc} performance is closely sensitive to the charge transfer processes at the TiO_2/dye/electrolyte interface,[36,37] which can be elucidated by electrochemical impedance spectroscopy (EIS).[38,39] Generally, the incorporation of long alkyl chains into organic push-pull sensitizers is regarded as an efficient approach to improve the dye layer morphology on TiO_2 and restrain charge recombination, thus remarkably increase the radius of the midsemicircle (in Nyquist plots) and move the phase angle peak (in Bode plots) to low frequency.[40,41]

As shown in Fig. 5a, under simulated AM1.5 solar light, the radius of the larger semicircle increases in the order of TTR1 < TTR2 < TTR3, indicating that the electron recombination resistance increases in the same order. This result is in agreement with the observed shift in the V_{oc} values. Compared with the DSSCs with CDCA coadsorbant, the TTR1-3 based DSSCs show smaller semicircle in absence of CDCA (Fig. S7), which is

corresponding to the decrease of the V_{oc} values as shown in Table 1 and Table 3. As shown in Fig.S2, evidently, the charge transfer resistance in the high-frequency region increases from TTR1 to TTR2 (TTR3), which is consistent with the higher V_{oc} value of TTR2 (TTR3) compared with that of TTR1. Therefore, the higher charge recombination rate may partly results in the existence of the wide gap (50mV) between the open-circuit voltages of TTR2 (TTR3) and TTR1.

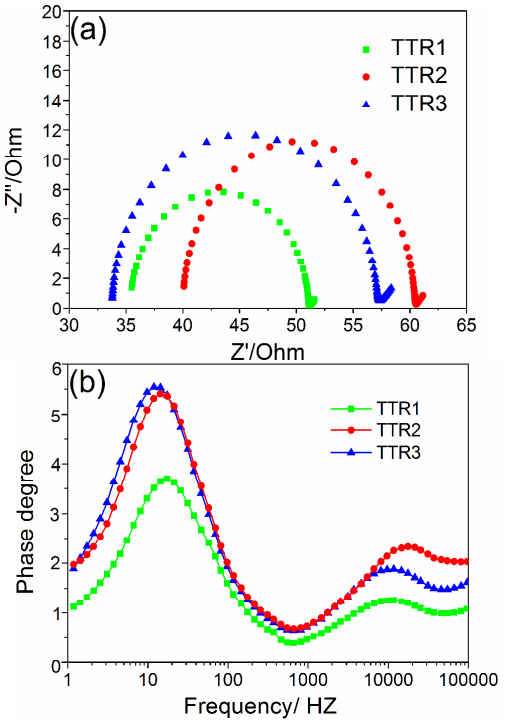

Fig. 5 EIS Nyquist (a) and Bode (b) plots for TTR1-3 based DSSCs with CDCA coadsorbant measured under illumination of 100 mW cm^{-2} simulated AM1.5 solar light.

Fig.5b shows the Bode plots of the DSSCs based on TTR1-3. All EIS Bode plots exhibit two-peak features for the frequency investigated. The peak at lower frequency corresponds to the charge transfer at the TiO_2/dye/electrolyte interface, which is related to the charge recombination rate and whose reciprocal is associated with the electron lifetime.[42] In Fig. 5b, the low frequency peak of TTR3 shows a lower frequency than those of TTR1 and TTR2, indicating that TTR3-based DSSC has longer electron lifetimes, which leads to a lower rate of charge recombination. The electron lifetime values is in the order of TTR1 < TTR2 < TTR3, likewise supporting the observed shift in the V_{oc} value.

3.7 Effects of sensitization ways for DSSCs

DSSCs based on single dye with different soaking time were investigated under irradiation of AM 1.5G full sunlight. Photocurrent-voltage (*J-V*) curves for these DSSCs without CDCA were presented in Fig. 6 and the exact results were summarized in Table 3.

As shown in Fig.6, the J_{sc} of TTR1-3 soaked for 16+16 h improves significantly compared with that of soaked for 16 and 32 h, which results from the fact that increasing the adsorption quantity (Table S2) enhances light harvesting ability. At the same soaking time, the V_{oc} of the DSSCs soaked twice in 32 h (16+16 h) are also superior to that soaked once in 32 h. We speculate that there are two adsorption types on the TiO_2 surface, namely, physical adsorption and chemical adsorption. For the former, after the first 16 h soaking (Fig. 7a), photoanode was rinsed with dichloromethane and dye molecules that were physical adsorbed were washed away, which resulted in vacancy on the TiO_2 surface, thus oxidation species in electrolyte, especially for I_3^- which possesses small size, was easy to approach photoanode and leading to the decrease in V_{oc} (Fig. 7a). As is shown in Fig.7b, the second 16 h bathing can not only prevent oxidation species from approaching photoanode, but also increase the adsorption quantity of dye molecules (Table S2), which gives rise to large V_{oc} and J_{sc}. The improvement of PCE is realized through re-sensitization, which provides a new sensitization method to improve the performance of DSSCs.

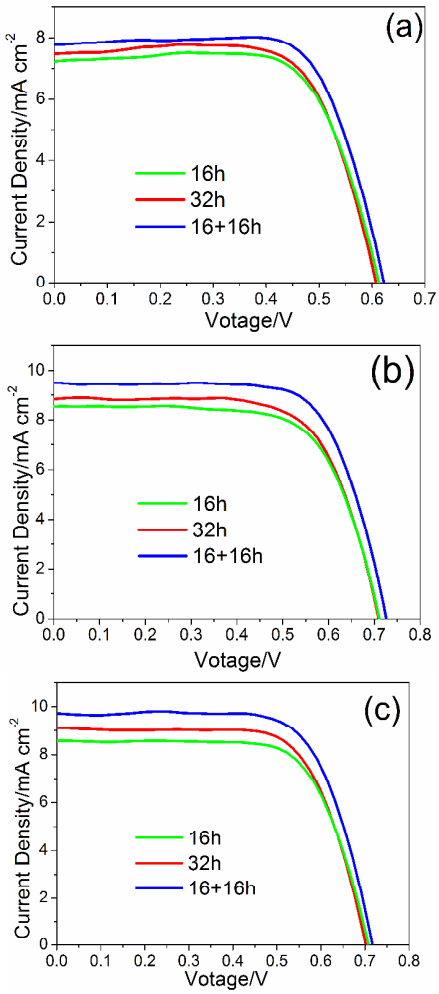

Fig. 6 Photocurrent density-voltage curves for the DSSCs based on TTR1-3 corresponding to (a), (b), and (c) under different soaking time.

Table 3 DSSC performance parameters of TTR1, TTR2 and TTR3.[a]

TTR1				
Soaking time	V_{oc}(V)	J_{sc}(mA cm^{-2})	*F.F.*%	η%
16h[a]	0.608	6.895	72	3.000
32h[b]	0.603	7.485	71	3.261
16+16h[c]	0.625	0.781	71	3.453
TTR2				
Soaking time	V_{oc}(V)	J_{sc}(mA cm^{-2})	*F.F.*%	η%
16h[a]	0.709	8.487	69	4.151
32h[b]	0.707	8.812	69	4.326
16+16h[c]	0.726	9.411	71	4.850
TTR3				
Soaking time	V_{oc}(V)	J_{sc}(mA cm^{-2})	*F.F.*%	η%
16h[a]	0.694	8.581	71	4.216
32h[b]	0.695	9.107	70	4.442
16+16h[c]	0.713	9.736	70	4.856

[a]The photocurrent–voltage characteristics were measured under soaking 16 h, 32 h and 16+16 h corresponding to the [a], [b] and [c].

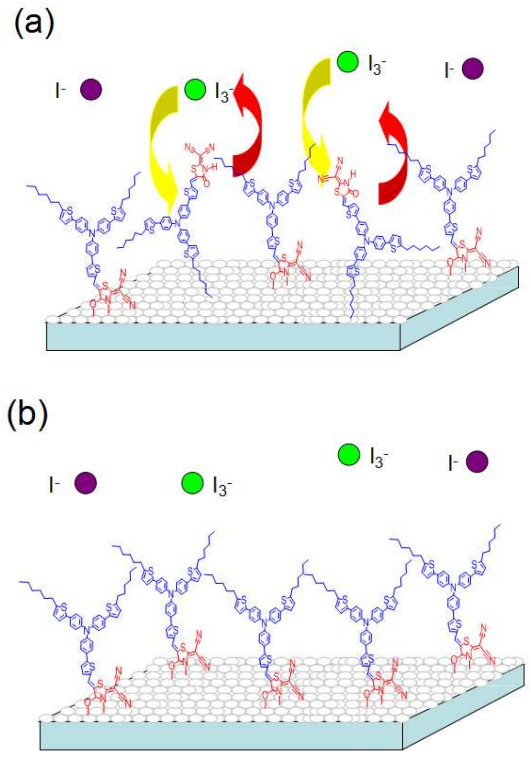

Fig. 7 (a) Schematic diagram of dealing for the first 16 h bathing. (b) Schematic diagram of dealing with following 16 h re-sensitization.

4. Conclusions

In this paper, three metal-free dyes (TTR1-3) that contain the triphenylamine moiety as an electron donor, thiophene ring as π-bridge, and 2-(1,1-dicyanomethylene)rhodanine (DCRD) as electron acceptor, have been successfully designed and synthesized. We investigated their photovoltaic properties to discuss the effects of introduction of different functional groups on the performance of the DSSCs. The overall PCE of the DSSCs based on TTR1-3 coadsorbant are 5.20% 5.71% and 6.30%, respectively. The DSSCs based on TTR2 and TTR3 showed higher J_{sc}, V_{oc}, and PCE values due to the introduction of a functional group to prevent aggregates and suppress recombination. In addition, we also researched the effect of sensitization ways for single dye on their photovoltaic performances. We found that, soaked twice in 32 h, the J_{sc} and V_{oc} were both obviously improved. These results provide a new approach for enhancing the photovoltaic performances of DSSCs based on single dye.

Acknowledgements

This work was supported by grants from the Natural Science Foundation of China (NO. 21371092; 91022011), the Natural Science Foundation of Jiangsu (No. BK20140986), and National Basic Research Program of China (2010CB923303).

Notes and references

[a]*State Key Laboratory of Coordination Chemistry, School of Chemistry and Chemical Engineering, Collaborative Innovation Center of Advanced Microstructures, Nanjing University, Nanjing 210093, P. R. China, E-mail: zhenghg@nju.edu.cn. Fax : 86-25-83314502.*
[b]*School of Chemical Engineering, Nanjing University of Science and Technology, Nanjing 210094, P. R. China, E-mail: xhju@mail.njust.edu.cn.*
[c]*State Key Laboratory of Materials-Oriented Chemical Engineering, College of Chemistry and Chemical Engineering, Nanjing University of Technology, Nanjing 210009, P. R. China, E-mail: zhouxf@njut.edu.cn*
[d]*Jiangsu Key Laboratory of Atmospheric Environment Monitoring and Pollution Control, School of Environmental Science and Engineering, Nanjing University of Information Science & Technology, Nanjing 210044, Jiangsu, P.R. China. E-mail: matchlessjimmy@163.com.*
†Electronic supplementary information (ESI) available: Experimental details of the EIS experiments and adsorption amount, cyclic voltammogram, synthesis of TTR1-3, FTIR spectrum of TTR1-3 power and absorbed on TiO_2, EIS Nyquist for single dye and density functional calculations of TTR1 and TTR2 are reported in the ESI.

1 B. O'Regan and M. Grätzel, *Nature*, 1991, **353**, 737.
2 A. Hagfeldt, G. Hagfeldt, L. C. Sun, L. Kloo and H. Pettersson, *Chem. Rev*., 2010, **110**, 6595.
3 J. F. Lu, S. S. Liu, H. Li, Y. Shen, J. Xu, Y. B. Cheng and M. K. Wang, *J. Mater. Chem. A*., 2014, **2**, 17551.
4 H. R. Li, K. W. Fu, A. Hagfeldt, M. Grätzel, S. G. Mhaisalkar and A. C. Grimdfale, *Angew. Chem. Int. Ed*., 2014, **53**, 4085.
5 Y. B. Li, H. F. Wang, H. M. Zhang, P. R. Liu, Y. Wang, W. Q. Fang, H. G. Yang, Y. Li and H. J. Zhao, *Chem. Commun*., 2014, **50**, 5569.
6 H. Wang, J. Li, F. Gong, G. Zhou and Z. S. Wang, *J. Am. Chem. Soc*., 2013, **135** , 12627.
7 T. Kinoshita, J. T. Dy, S. Uchida, T. Kubo and H. Segawa, *Nature Photonics,* 2013, **7**, 535.
8 A. Yella, H. W. Lee, H. N. Tsao, C. Yi, A. K. Chandiran, M. K. Nazeeruddin, E. W. Diau, C. Y. Yeh, S. M. Zakeeruddin and M. Grätzel, *Science*, 2011, **334**, 629.
9 S. Mathew, A. Yella, P. Gao, R. H. Baker, B. F. E. Curchod, N. A. Astani, I. Tavernelli, U. Rothlisberger, M. K. Nazeeruddin and M. Grätzel, *Nature Chemistry*, 2014, **6**, 242.

10 H. Choi, M. Shin, K. Song, M. S. Kang, Y. J. Kang and J. Ko, *J. Mater. Chem. A.*, 2014, **2**, 12931.

11 B. Liu, Q. B. Liu, D. You, X. Y. Li, Y. Naruta and W. H. Zhu, *J. Mater. Chem*., 2012, **22**, 13348.

12 A. Kovyrshin, F. D. Angelis and J. Neuqebauer, *Phys. Chem. Chem. Phys.*, 2012, **14**, 8608.

13 T. Sudyoadsuk, S. Pansay, S. Morada, P. Rattanawan, S. Namuangruk, T. Kaewin, S. Jungsuttiwong and V. Promarak, *Eur. J. Org. Chem*., 2013, **23**, 5051.

14 S. Aqrawal, N. J. English, K. R. Thampi and J. M. D. Macelroy, *Phys. Chem. Chem. Phys.*, 2012, **14**, 12044.

15 Y. Hua, S. Chang, J. He, C. S. Zhang, J. Z. Zhao, T. Chen, W. Y. Wong, W. K. Wong and X. J. Zhu, *Chem. Eur. J.* 2014, **20**, 6300.

16 Z. Fang, A. A. Eshbaugh and K. S. Schanze, *J. Am. Chem. Soc.,* 2011, **133**, 3063.

17 X. F. Lu, X. W. Jia, Z. S. Wang and G. Zhou, *J. Mater. Chem. A*., 2013, **1**, 9697.

18 K. C. D. Robson, K. Hu, G. J. Meyer and C. P. Berlinguette, *J. Am. Chem. Soc*., 2013, **135**, 1961.

19 M. D. Zhang, H. X. Xie, X. H. Ju, L. Qin, Q. X. Yang, H. G. Zheng and X. F. Zhou, *Phys. Chem. Chem. Phys*., 2013, **15**, 634.

20 L. L. Tan, J. F. Huang, Y. Shen, L. M. Xiao, J. M. Liu, D. B. Kuang and C. Y. Su, *J. Mater. Chem. A*, 2014, **2**, 8988.

21 J. F. Huang, J. M. Liu, L. L. Tan, Y. F. Chen, Y. Shen, L. M. Xiao, D. B. Kuang and C. Y. Su, *Dye and Pigments*, 2015, **114**, 18.

22 J. Y. Mao, N. N. He, Z. J. Ning, Q. Zhang, F. L. Guo, L. Chen, W. J. Wu, J. L. Hua and H. Tian, *Angew. Chem. Int. Ed.*, 2012, **51**, 9873.

23 H. S. He, A. Gurung and L. P. Si, *Chem. Commun*., 2012, **48**, 5910.

24 Y. Ooyama, S. Inoue, T. Nagano, K. Kushimoto, J. Ohshita, I. Imae, K, Komaguchi and Y. Harima, *Angew. Chem. Int. Ed.*, 2011, **123**, 7567.

25 C. Teng, X. C. Yang, S. F. Li, M. Cheng, A. Hanfeldt, L. Z. Wu and L. C. Sun, *Chem. Eur. J*., 2010, **16**, 13127.

26 P. G. Bomben, T. J. Gordon, E. Schott and C. P. Berlinguette, *Angew. Chem. Int. Ed.*, 2011, **50**, 10682.

27 L. F. Lai, C. L. Ho, Y. C. Chen, W. J. Wu, F. R. Dai, C. H. Chui, S. P. Huang, K. P. Guo, J. T. Lin, H. Tian, S. H. Yang and W. Y. Wong, *Dyes and Pigments*, 2013, **96**, 516.

28 Q. Wang, S. Ito, M. Grätzel, F. Fabregat-Santiago, I. Mora-Sero, J. Bisquert, T. Bessho and H. Imai, *J. Phys. Chem. B.*, 2006, **110**, 25210.

29 M. J. Frisch, et al., Gaussian 09, Revision A.02, Gaussian, Inc. Wallingford, CT, 2009.

30 J. J. P. Stewart, *J. Mol. Model*., 2007, **13**, 1173.

31 M. C. Zerner, Reviews of Computational Chemistry, **VCH**, New York, 1991, p. 313.

32 B. G. Kim, K. Chung and J. Kim, *Chem. Eur. J.,* 2013, **19**, 5220.

33 B. A. Greeg, F. Pichot, S. Ferrere and C. L. Field, *J. Phys. Chem. B*., 2001, **105**, 1422.

34 J. B. Lynch, P. L. Fast, M. Harris and D. G. Truhlar, *J. Phys. Chem. A.,* 2000, **104**, 4811.

35 J. B. Yang, F. L. Guo, J. L. Hua, X. Li, W. J. Wu, Y. Qu and H. Tian, *J. Mater. Chem.,* 2012, **22**, 24356.

36 A. Hagfeldt, and M. Grätzel, *Chem. Rev*., 1995, **95**, 49.

37 K. L. Wu, C. H. Li, C. H. Y. Chi, Y. Clifford, L. Cabau, E. Palomares, Y. M. Cheng, H. A. Pan, and P. T. Chou, *J. Am. Chem. Soc.,* 2012, **134**, 7488.

38 J. J. H. Pijpers, R. Ulbricht, R. Derossi, J. N. H. Reek and M. Bonn, *J. Phys. Chem. C.*, 2011, **115**, 2578.

39 Q. Wang, J. E. Moser, and M. Grätzel, *J. Phys. Chem. B.,* 2005, **109**, 14945.

40 R. Kern, R. Sastrawan, J. Ferber, R. Stangl and J. Luther, *Electrochim. Acta.*, 2002, **47**, 4213.

41 A. S. Hart, C. B. KC, H. B. Gobeze, L. R. Sequeira and F. D'Souza, *Appl. Mater. Interfaces,* 2013, **5**, 5314.

42 L. Y. Lin, C. H. Tsai, K. T. Wong, T. W. Huang, L. Hsieh, S. H. Liu, H. W. Lin, C. C. Wu, S. H. Chou, S. H. Chen and A. I. Tsai, *J. Org. Chem*., 2010, **75**, 4778.

Graphical Abstract

Improvement of Dye-Sensitized Solar Cells' Performance through Introducing Different Heterocyclic Groups to Triarylamine Dyes

Ze-Min Ju, Hai-Lang Jia, Xue-Hai, Ju, Xing-Fu Zhou, Zhi-Qiang Shi, He-Gen Zheng* and Ming-Dao Zhang*

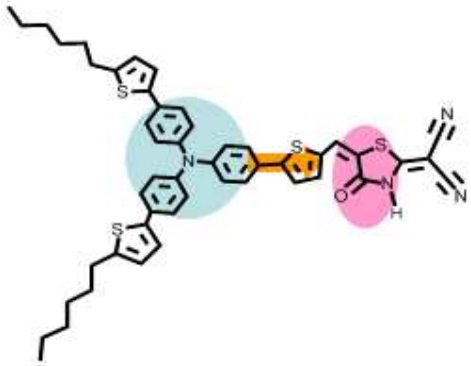

The overall power conversion efficiency (PCE) of DSSCs based on TTR1-3 with chenodeoxycholic acid (CDCA) coadsorbant are 5.20%, 5.71% and 6.30%, respectively, and the value of TTR3 is close to that of N719 (6.62%).